


Exhibit 16

SOURCE
DATATRANSPARENT
PROCESSEMBO
reports

Article

Fusobacterium nucleatum promotes colorectal cancer by inducing Wnt/ β -catenin modulator Annexin A1

Mara Roxana Rubinstein^{1,†}, Jung Eun Baik^{1,†}, Stephen M Lagana², Richard P Han³, William J Raab², Debashis Sahoo⁴, Piero Dalerba^{2,5,6,7}, Timothy C Wang^{6,7} & Yiping W Han^{1,6,7,8,*} 

Abstract

Fusobacterium nucleatum, a Gram-negative oral anaerobe, is a significant contributor to colorectal cancer. Using an *in vitro* cancer progression model, we discover that *F. nucleatum* stimulates the growth of colorectal cancer cells without affecting the pre-cancerous adenoma cells. Annexin A1, a previously unrecognized modulator of Wnt/ β -catenin signaling, is a key component through which *F. nucleatum* exerts its stimulatory effect. Annexin A1 is specifically expressed in proliferating colorectal cancer cells and involved in activation of Cyclin D1. Its expression level in colon cancer is a predictor of poor prognosis independent of cancer stage, grade, age, and sex. The FadA adhesin from *F. nucleatum* up-regulates Annexin A1 expression through E-cadherin. A positive feedback loop between FadA and Annexin A1 is identified in the cancerous cells, absent in the non-cancerous cells. We therefore propose a “two-hit” model in colorectal carcinogenesis, with somatic mutation(s) serving as the first hit, and *F. nucleatum* as the second hit exacerbating cancer progression after benign cells become cancerous. This model extends the “adenoma-carcinoma” model and identifies microbes such as *F. nucleatum* as cancer “facilitators”.

Keywords Annexin A1; colorectal cancer; FadA; *Fusobacterium nucleatum*; two-hit model

Subject Categories Cancer; Microbiology, Virology & Host Pathogen Interaction; Signal Transduction

DOI 10.15252/embr.201847638 | Received 21 December 2018 | Revised 23 January 2019 | Accepted 29 January 2019 | Published online 4 March 2019

EMBO Reports (2019) 20: e47638

Introduction

Colorectal cancer (CRC) is the second leading cause of cancer death in the United States, affecting 1 in 20 individuals [1]. CRC has long been recognized to result from host mutations that accumulate over time, developing from pre-cancerous adenomatous polyps into adenocarcinoma over approximately 10 years [2]. Advancements in microbial detection technology and human microbiome research have revolutionized our understanding of a wide spectrum of diseases, including CRC [3–7]. Numerous recent studies have reported that the anaerobic Gram-negative oral commensal bacterium, *Fusobacterium nucleatum*, plays a significant role in colorectal carcinogenesis [8–14]. *F. nucleatum* has been detected in ~10–90% CRC tissues, with higher prevalence in the proximal than distal colon [15–17]. It is often associated with advanced disease, chemo-resistance, metastasis, and poor prognosis [14,18–20]. A few studies have supported a causal role of *F. nucleatum* in CRC [10,12,14,21], but detailed mechanistic investigations are scarce. We have reported previously that *F. nucleatum* promotes CRC growth through its unique FadA adhesin, which binds to E-cadherin (CDH1) and activates Wnt/ β -catenin signaling, causing nuclear translocation of β -catenin and overexpression of inflammatory genes, Wnt genes, and oncogenes c-Myc and Cyclin D1 (CCND1) [12]. Binding of FadA to E-cadherin requires both the intact pre-FadA consisting of 129 amino acid residues and mFadA of 111 amino acid residues without the signal peptide. Together, they form the FadAc complex [12,22]. FadA was unable to promote growth of non-cancerous HEK293 cells even in the presence of E-cadherin [12]. This observation raised the question whether *F. nucleatum*-induced growth stimulation is specific for CRC. We report here that *F. nucleatum* selectively stimulates the growth of colorectal cancerous cells through activation of Annexin A1 (ANXA1), a member of

1 Division of Periodontics, College of Dental Medicine, Columbia University, New York, NY, USA

2 Department of Pathology and Cell Biology, Vagelos College of Physicians & Surgeons, Columbia University, New York, NY, USA

3 The Horace Mann School, Bronx, NY, USA

4 Department of Computer Science and Engineering, University of California San Diego, San Diego, CA, USA

5 Columbia Stem Cell Initiative, Columbia University, New York, NY, USA

6 Division of Digestive and Liver Diseases, Columbia University, New York, NY, USA

7 Herbert Irving Comprehensive Cancer Center, Columbia University, New York, NY, USA

8 Department of Microbiology and Immunology, Vagelos College of Physicians & Surgeons, Columbia University, New York, NY, USA

*Corresponding author. Tel: +1 212 342 1790; E-mail: ywh2102@cumc.columbia.edu

[†]These authors contributed equally to this work

the Annexin family of Ca^{2+} -dependent phospholipid-binding proteins [23]. Annexin A1 has a molecular weight of 35–40 kDa and can be found in nucleus, cytoplasm, and plasma membrane of various cell types. ANXA1 is involved in a variety of biological processes and has been postulated to be either a tumor suppressor or promoter depending on the tumor types [24,25]. Increased expression of Annexin A1 in CRC has been reported [26,27], but its role remains unclear. We discover that Annexin A1 is a previously unrecognized Wnt/ β -catenin modulator and a critical growth stimulator of CRC, whose expression is increased in proliferating CRC cells, but not in non-proliferating or non-cancerous cells. Given the lack of stimulation of non-cancerous cells by *F. nucleatum*, we propose a “two-hit” model, whereby *F. nucleatum* becomes a “facilitator” of cancer progression only after the benign cells progress to a malignant phenotype.

Results

Fusobacterium nucleatum selectively stimulates the growth of colorectal cancerous cells

In order to determine the specificity of *F. nucleatum*-mediated growth stimulation, we tested the effects of *F. nucleatum* strain WAL12230 on the PC-9 lung cancer cells, 22RV1 prostate cancer cells, and MCF7 breast cancer cells, all of which expresses E-cadherin, as well as UMUC3 bladder cancer cells, which does not express E-cadherin [28–31] (Fig EV1A). No growth stimulation was detected; on the contrary, *F. nucleatum* inhibited the proliferation of PC-9, 22RV1, and UMUC3 cells, presumably due to toxic effects (Fig 1A).

We then tested *F. nucleatum* stimulation of the colonic cells, utilizing a CRC progression model consisting of a series of cell lines sequentially derived from a human colonic adenoma [32]. AA/C1 is a slow-growing non-cancerous adenoma cell line with low colony-forming efficiency. Following treatment with 1 mM sodium butyrate, it gave rise to the AA/C1/SB cell line, which grows faster with increased colony-forming efficiency, but remains non-tumorigenic in mice. The AA/C1/SB cells were further mutagenized with *N*-methyl-*N'*-nitro-*N*-nitrosoguanidine to produce a tumorigenic (cancerous) cell line, AA/C1/SB/10C [32]. *F. nucleatum* 12230 accelerated the growth of the AA/C1/SB/10C cells (from now on referred to as “10C”), but not of the non-tumorigenic AA/C1 or AA/C1/SB (from now on referred to as “SB”) cells (Fig 1A). As with our previous report, the growth stimulation was mediated predominantly through FadA although the *fadA*-deletion mutant US1 retained a weak stimulatory effect, suggesting additional component(s) may be involved [12]. Although all cell lines tested with *F. nucleatum* 12230 expressed increased levels of proinflammatory markers, only the cancerous 10C cells exhibited elevated expression of the oncogene Cyclin D1, consistent with growth stimulation (Fig EV1B).

Fusobacterium nucleatum binds and invades cancerous cells more efficiently due to Annexin A1

F. nucleatum 12230 bound 75% more and invaded 150% more efficiently to the cancerous 10C cells, as compared to its non-cancerous predecessor SB (Fig 1B). These results were consistent with our previous finding that the *fadA* gene levels (and *F. nucleatum*) were

significantly higher in the human colorectal carcinoma tissues than in the adenoma tissues [12]. The results also suggest that 10C and SB may differ in their membrane components, which might explain the differential binding by *F. nucleatum*.

Previous comparative proteomic analysis revealed two membrane proteins that were increased in 10C compared to SB: Annexin A1 and Villin 1 (*VIL1*) [33]. Down-regulation of Annexin A1 in the 10C cells by siRNA effectively reduced *F. nucleatum* binding and invasion, in a similar manner as suppression of *CDH1* (Fig 1B), whereas knock-down of *VIL1* had no effect (Fig 1C). Transfection of *ANXA1* into SB cells significantly increased *F. nucleatum* binding and invasion (Fig 1B). These results indicate that Annexin A1 plays an important role in *F. nucleatum* interaction with the cancerous 10C cells. Hence, from this point onward, our investigation focused on Annexin A1.

Annexin A1 is an independent CRC prognosis biomarker

To examine *ANXA1* expression in CRC biology in humans, we tested for their association with recurrence rates in a clinical database annotated with microarray gene-expression measurements from 466 primary colon carcinomas [34]. The association was first tested using Kaplan–Meier survival curves, using three different approaches for patient stratification: (i) based on the median of *ANXA1* mRNA expression levels (Fig 2A); (ii) based on the quartile distribution of *ANXA1* mRNA expression levels (Fig 2B); and (iii) based on expression thresholds calculated using the StepMiner algorithm (Fig 2C), as previously described [35,36]. High levels of *ANXA1* mRNA expression were associated with a statistically significant reduction in disease-free survival (DFS) rates, irrespective of the method used for the stratification ($P < 0.001$, log-rank test). Differences in *ANXA1* mRNA expression levels did not appear to correlate with differences in each tumor’s relative content of epithelial cells (i.e., tumor cell density) as revealed by the lack of visual correlations with the epithelial cell marker Desmoplakin (*DSP*). Importantly, the association between high levels of *ANXA1* mRNA expression and increased risk of recurrence remained statistically significant in a series of multivariate analyses (Cox proportional hazards method) that excluded clinical stage, pathological grade, age, and sex as possible confounding variables, even after modeling *ANXA1* expression as a continuous variable (Table 1). The hazard ratio (HR) for disease recurrence associated with increased *ANXA1* expression levels was 1.44 (95% CI 1.24–1.68; $P < 0.001$) when tested alongside clinical stage, age, and sex across the full patient cohort ($n = 466$), and 1.56 (95% CI 1.21–2.02; $P < 0.001$) when tested alongside clinical stage, pathological grade, age, and sex in the patient subgroup annotated with pathological grade ($n = 216$). These analyses demonstrate that *ANXA1* is a novel colon cancer prognostic biomarker.

Annexin A1 is a CRC growth factor specifically expressed in proliferating cancerous cells

We found Annexin A1 was selectively expressed in proliferating cancerous cells. In 10C and human CRC cells, HCT116, DLD1, and RKO, *ANXA1* gene expression was significantly higher in the non-confluent than confluent state, despite that very little was expressed in RKO (Fig 3A). Immunofluorescence staining revealed that Annexin A1 was expressed on the outer layer of the growing mass

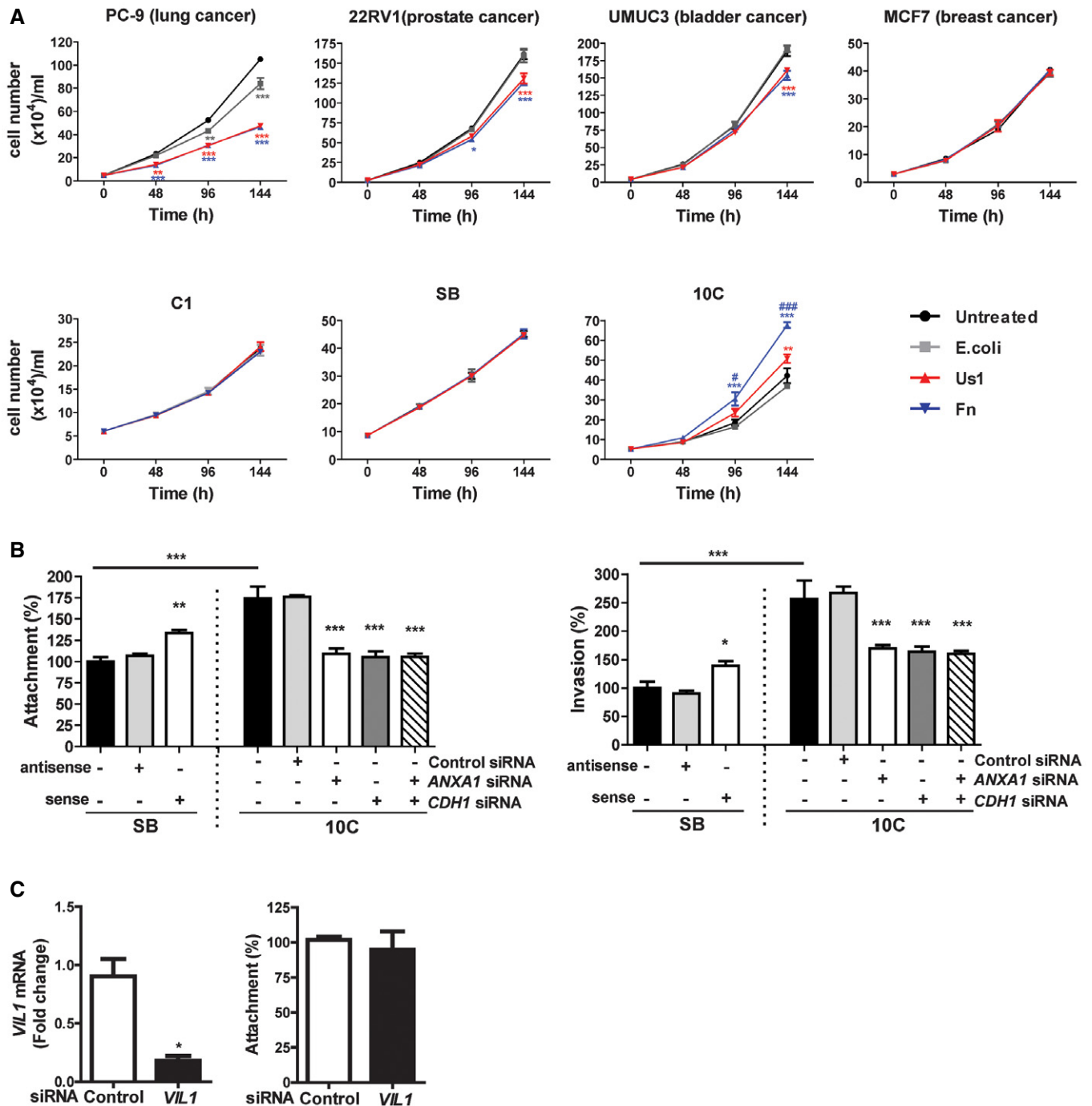


Figure 1. *Fusobacterium nucleatum* preferentially binds, invades, and stimulates the growth of cancerous colorectal cells via Annexin A1.

A Lung cancer cells PC-9, prostate cancer cells 22RV1, bladder cancer cells UMUC3, breast cancer cells MCF-7, colonic adenoma-derived non-cancerous cells AA/C1 (aka C1) and AA/C1/SB (aka SB), or cancerous cells AA/C1/SB/10C (aka 10C) were incubated with wild-type *F. nucleatum* 12230 (*Fn*), the *fadA*-deletion mutant US1 (US1), or *E. coli* DH5 α (*E. coli*) at multiplicity of infection (MOI) of 1,000:1. Cell numbers are mean values \pm SEM. The experiment was performed in triplicates and repeated three times. * P < 0.05, ** P < 0.01, *** P < 0.001, compared to untreated controls; [#] P < 0.05, ^{###} P < 0.001, compared to US1-treated cells (two-way ANOVA).

B Attachment (left panel) and invasion (right panel) of wild-type *F. nucleatum* 12230 (Fn) to the non-cancerous SB cells, either untreated or transfected with antisense or sense *ANXA1*, and to the cancerous 10C cells, either untreated or transfected with control or *ANXA1*- or *CDH1*-specific siRNA or both (MOI 50:1). *F. nucleatum* attachment and invasion to the untreated SB cells were designated as 100%, respectively; all other values were expressed as relative to those obtained with untreated SB. Data are mean values \pm SEM. The experiment was performed in triplicates and repeated four times. **P* < 0.05, ***P* < 0.01, and ****P* < 0.001 (one-way ANOVA).

C Left panel: qPCR analysis of Villin 1 (*VIL1*) mRNA levels in 10C cells treated with control siRNA or *VIL1*-specific siRNA, demonstrating knockdown of Villin 1. Right panel: Attachment of *F. nucleatum* 12230 to 10C cells treated with control siRNA or *VIL1*-specific siRNA. Data are mean values \pm SD. The experiment was performed in triplicates and repeated twice. * $P < 0.05$ (Student's *t*-test).

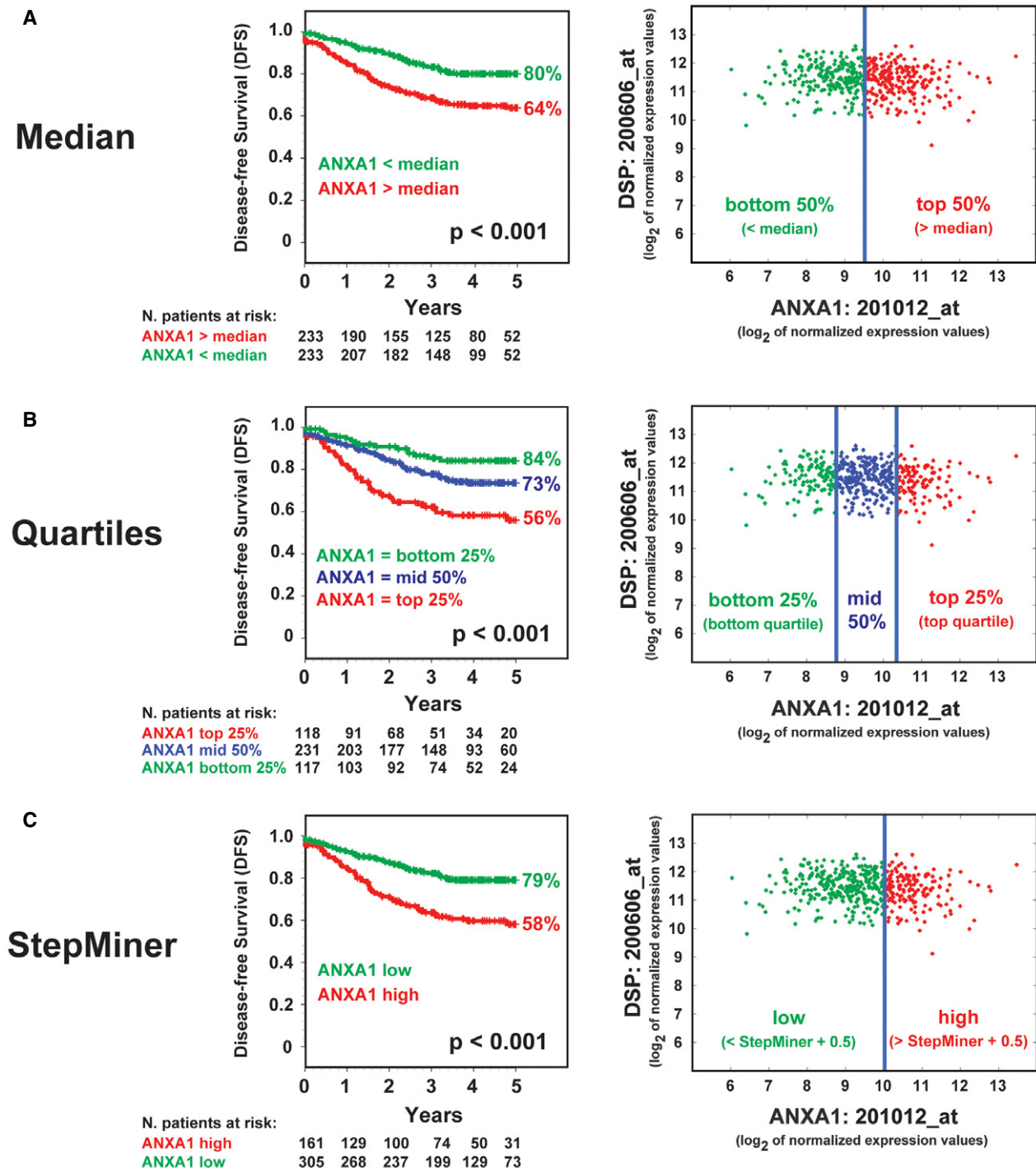


Figure 2. Annexin A1 is a novel colon cancer prognosis marker.

A–C Relationship between *ANXA1* mRNA expression levels and disease-free survival (DFS) in colon cancer patients. The relationship between *ANXA1* mRNA expression levels and DFS was investigated in a database of 466 primary colon carcinomas, assembled by pooling four independent gene-expression array datasets from the NCBI-GEO online repository (GSE14333, GSE17538, GSE31595, GSE37892), as previously described [34]. The association between *ANXA1* expression levels and DFS was tested using Kaplan–Meier survival curves, after patient stratification in groups with high, medium, and low *ANXA1* expression, using three different methods: (A) based on the median of *ANXA1* mRNA expression levels (high 50% versus low 50%); (B) based on the quartile distribution of *ANXA1* mRNA expression levels (high 25% versus middle 50% versus low 25%); and (C) based on *ANXA1* mRNA expression thresholds calculated using the StepMiner algorithm (low versus high), as previously described [35,36]. Overall, high *ANXA1* mRNA expression levels were associated with a statistically significant reduction in DFS ($P < 0.001$, log-rank test), irrespective of the method used for the stratification. Differences in *ANXA1* mRNA expression levels did not appear to correlate with differences in each tumor's relative content of epithelial cells in the analyzed biospecimens (i.e., tumor cell density) as revealed by the lack of visual correlations with the epithelial cell marker Desmoplakin (*DSP*).

Table 1. Relationship between ANXA1 mRNA expression levels and risk of recurrence in colon cancer patients.

	Cox proportional hazards model					
	Univariate			Multivariate		
	HR	95% CI	P-value	HR	95% CI	P-value
All patients (n = 466)						
ANXA1 ^a	1.46	1.25–1.71	< 0.001***	1.44	1.24–1.68	< 0.001***
Stage (I–IV)	3.47	2.62–4.59	< 0.001***	3.73	2.74–5.09	< 0.001***
Age ^a	0.99	0.97–1.00	0.06	1.00	0.98–1.01	0.75
Sex (M/F) ^b	1.07	0.89–1.28	0.49	1.05	0.88–1.27	0.58
Patients annotated with information on tumor grade (n = 216)						
ANXA1 ^a	1.48	1.18–1.87	< 0.001***	1.56	1.21–2.02	< 0.001***
Stage (I–IV)	3.13	2.14–4.60	< 0.001***	3.63	2.31–5.70	< 0.001***
Grade (G1–G3)	1.63	0.94–2.82	0.08	1.02	0.58–1.79	0.95
Age ^a	0.99	0.97–1.01	0.20	1.00	0.98–1.02	0.85
Sex (M/F) ^b	1.15	0.88–1.51	0.32	1.16	0.86–1.55	0.33

CI, confidence interval; HR, hazard ratio.

The relationship between ANXA1 mRNA expression levels and risk of recurrence was investigated in a database of 466 primary colon carcinomas, obtained by assembling four independent gene-expression array datasets downloaded from the NCBI-GEO online repository (GSE14333, GSE17538, GSE31595, GSE37892), as previously described [34]. The association between ANXA1 mRNA expression levels and risk of recurrence was tested using both univariate and multivariate analyses based on the Cox proportional hazards method, where ANXA1 mRNA expression levels were modeled as a continuous variable. Overall, higher ANXA1 mRNA expression levels were associated with a statistically significant increase in the risk of recurrence when using univariate analysis, in both the whole database (n = 466; $P < 0.001$) and the subset of patients annotated with information on the pathological grading of the tumors (n = 216; $P < 0.001$).

Importantly, the association remained significant also in a multivariate analysis aimed at excluding possible confounding effects from clinical stage, pathological grade, age, or sex, both when tested across the whole database (n = 466; $P < 0.001$) and when tested in the subset of patients annotated for the pathological grading of the respective tumors (n = 216; $P < 0.001$). Hazard ratios (HRs) were tested for statistical significance (null hypothesis: HR=1) using the Wald test.

^aANXA1 mRNA levels and age modeled as a continuous variable.

^bM/F: male versus female.

*** $p < 0.001$.

of cancerous 10C cells (Fig 3B; Movie EV1). In contrast, Annexin A1 expression in SB remained at low levels, unaffected by cell density (Fig 3B).

Using ANXA1-specific siRNA, we were able to inhibit its expression (Fig EV2A). This led to inhibition of the growth of cancerous 10C, HCT116, DLD1, SW480, and HT29, but not the non-cancerous SB, or the CRC cells RKO, which expressed the lowest level of ANXA1 (Fig 3C). Transfection of ANXA1 into SB and RKO significantly stimulated their growth (Figs 3D and EV2B). Equal numbers of HCT116 cells transfected with control or ANXA1-specific siRNA were then injected subcutaneously and bilaterally into nude mice. Suppression of ANXA1 significantly attenuated tumor growth compared to controls (Fig 3E). Similar results were obtained with DLD1 (Fig EV2C). As no *F. nucleatum* was included in these experiments, the results demonstrate that Annexin A1 is a critical growth factor for CRC, regardless of *F. nucleatum*.

***Fusobacterium nucleatum* induces Annexin A1 expression in cancerous cells through FadA and E-cadherin**

We investigated the relationship between *F. nucleatum* and Annexin A1 and found *F. nucleatum* induced ANXA1 gene expression in the cancerous 10C, HCT116, and DLD1 cells, but not in the non-cancerous SB cells (Fig 4A). The induction required FadA, because the *fadA*-deletion mutant US1 was defective, and purified FadA induced Annexin A1 in a dose-dependent manner (Fig 4A and B). Of note, similar induction was detected upon re-analysis of

a recently published, publicly available RNA-seq dataset [14] that contains gene-expression data from human CRC cells HT29 incubated with a different strain, *F. nucleatum* ATCC 25586 (Fig EV3A). Taken together, these consistent observations indicate that ANXA1 overexpression can be interpreted as a common response of CRC cells to *F. nucleatum*, across different cell lines and bacterial strains.

We have shown previously that FadA binds to E-cadherin on CRC cells [12]. Therefore, we examined the interactions between FadA, E-cadherin, and Annexin A1. Induction of Annexin A1 expression by FadA was mediated through E-cadherin (Fig 4C) despite the fact that *F. nucleatum* did not affect E-cadherin expression at the transcriptional level (Fig EV3B). The induced Annexin A1 localized at the outer layer of the cell mass (Fig 4D), consistent with the observation in Fig 3B. No Annexin A1 was induced in the non-cancerous SB cells by *F. nucleatum* (Fig 4D), suggesting that the induction was specific for the cancerous cells.

FadA, E-cadherin, Annexin A1, and β -catenin form a complex in cancerous cells

Western blot analysis demonstrated a coordinated increase in E-cadherin, Annexin A1, and β -catenin protein expression with increased FadA binding over time (Fig 5A), suggesting possible interactions between these components. All four components could be co-immunoprecipitated, further supporting the formation of a multi-component complex (Fig 5B and C).

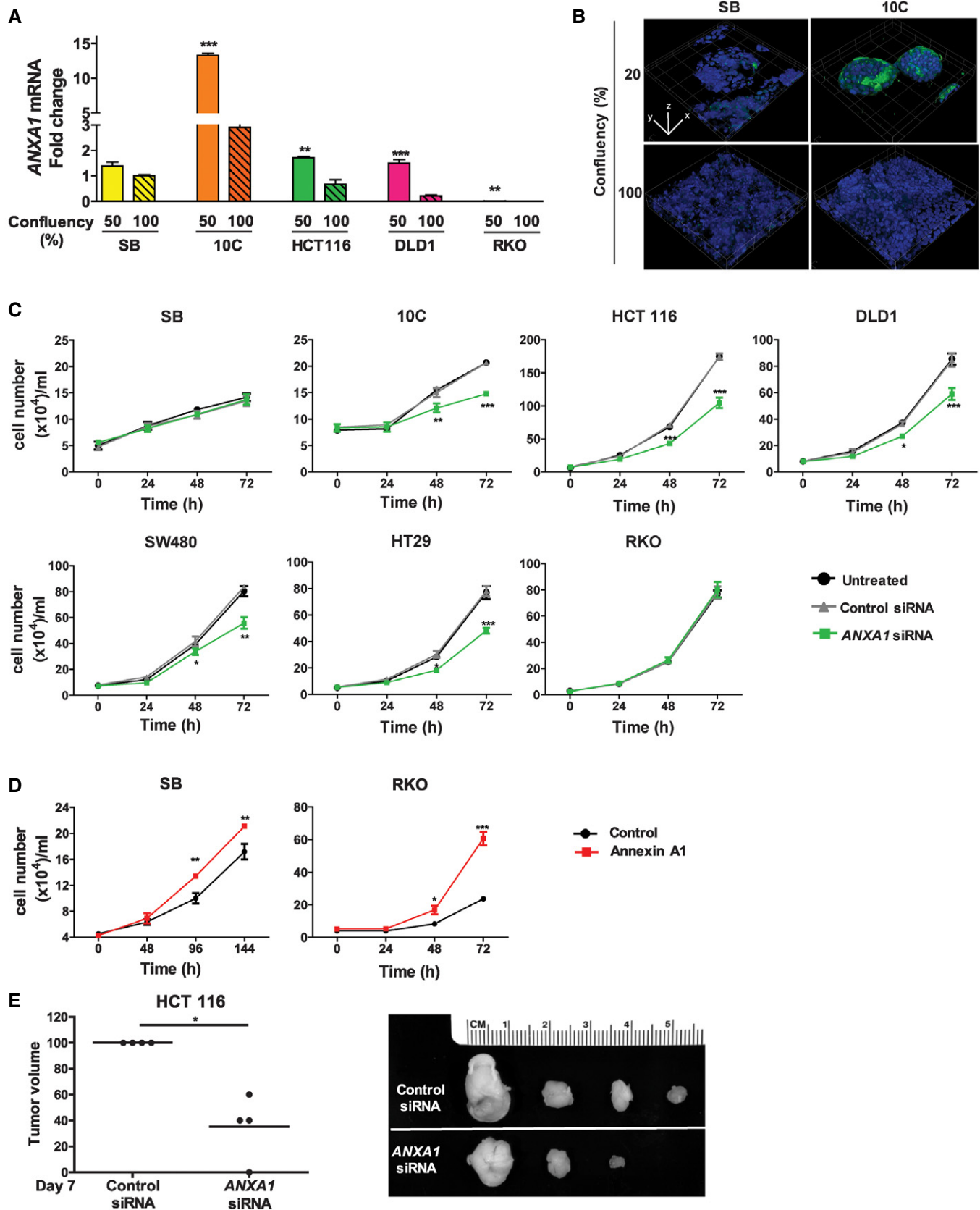


Figure 3.

Figure 3. Annexin A1 is a novel CRC growth factor selectively expressed in proliferating cancerous colorectal cells.

- A Real-time qPCR analysis of *ANXA1* expression using mRNA extracted from the non-cancerous SB, cancerous 10C, and human CRC cell lines HCT116, DLD1, and RKO, each grown to 50 or 100% confluency. All results were normalized to the *ANXA1* mRNA levels in SB cells of 100% confluency, which was designated as 1. Data are mean values \pm SEM. The experiment was performed in triplicates and repeated twice. $**P < 0.01$ and $***P < 0.001$ (Student's *t*-test).
- B Confocal microscopy analysis of SB and 10C cells grown to 20% (top panels) or 100% (bottom panels) confluency followed by immunofluorescence staining of Annexin A1 (green). The nuclei were stained with DAPI (blue). A series of 20–50 consecutive images in the *z*-axis were stacked together to generate the 3D figure at 400 \times magnification. Annexin A1 is most abundantly expressed on the outer layer of 20% confluent 10C (also see Movie EV1), compared to 100% confluent 10C, or SB of either confluency. Scale bars, *x* = 1 μ m, *y* = 1 μ m, *z* = 1.6 μ m. The experiment was repeated at least twice.
- C Cell proliferation assay of adenoma-derived non-cancerous SB and cancerous 10C and human CRC cell lines HCT116, DLD1, SW480, HT29, and RKO either untreated (black lines) or following treatment with control siRNA (gray lines) or *ANXA1*-specific siRNA (green lines). Data are mean values \pm SEM. The experiment was performed in triplicates and repeated three times. $*P < 0.05$, $**P < 0.01$, and $***P < 0.001$, compared to the untreated cells (two-way ANOVA).
- D Cell proliferation assay of SB (left panel) and RKO (right panel) cells transfected with *ANXA1* (red line), as compared to the control cells (black lines). Data are mean values \pm SEM. The experiment was performed in triplicates and repeated three times. $*P < 0.05$, $**P < 0.01$, and $***P < 0.001$ (two-way ANOVA).
- E Xenografted tumor growth in nude mice following subcutaneous and bilateral inoculation of HCT116 cells transfected with control siRNA or *ANXA1*-specific siRNA (*n* = 4). The tumor volumes were measured after 7 days postinjection (left panel). For each mouse, the tumor resulting from *ANXA1*-specific siRNA-treated cells was normalized to that from control siRNA-treated cells, which was designated 100%. The line represents the average. $*P < 0.05$ (paired *t*-test). The individual tumor pairs are shown on the right panel: top, tumors arising from control siRNA-treated cells; bottom, tumors arising from *ANXA1*-specific siRNA-treated cells.

Analysis by confocal microscopy confirmed that *F. nucleatum* and FadAc co-localized with E-cadherin and Annexin A1 in 10C and DLD1 cells on the cell membranes, as well as inside the cells (Figs 5D and E, and EV4). This is consistent with our previous reports that FadAc binds vascular endothelial (VE)-cadherin and E-cadherin causing them to internalize [12,37]. It should be noted that, compared to those incubated with mFadA or BSA, 10C cells incubated with FadAc exhibited not only increased expression of Annexin A1, but also enhanced co-localization of E-cadherin and Annexin A1, consistent with Fig 4D.

A positive feedback loop between FadA and Annexin A1 in cancerous cells

When *F. nucleatum* was incubated with the 10C cells, it exhibited preferential binding to Annexin A1-positive cells, starting at as early as 5 min of incubation, whereas slight preference for Annexin A1-negative cells was detected in SB (Fig 6A and B, compare solid and clear bars). Upon incubation of *F. nucleatum* with 10C cells, Annexin A1 expression increased with time, and so did *F. nucleatum* binding to the cells (Fig 6B). Similar observations were made with DLD1 and HCT116 cells (Fig 6C and D). The increase of Annexin A1 protein levels and binding of *F. nucleatum* were consistent with the kinetics of transcriptional activation (compare Figs 4A and 6). These results suggest a positive feedback loop in which *F. nucleatum* induces Annexin A1 expression in the cancerous cells, which in turn enhances bacterial binding. The *fadA*-deletion mutant US1 did not induce Annexin A1 expression because the amount of Annexin A1-positive cells did not change over time. However, US1 also exhibited preferential binding to Annexin A1-positive cells (Fig 6B–D), indicating Annexin A1 may mediate additional *F. nucleatum* component(s) to bind to the cancer cells.

FadA and Annexin A1 co-express in colorectal tumors in mice and humans

To examine the correlation between FadA and Annexin A1 *in vivo*, we utilized the *Apc*^{min/+} mice, which carry a mutation in one copy of the tumor suppressor *APC* gene and develop spontaneous tumors in the small intestine and colon. C57BL/6 *Apc*^{min/+} mice inoculated with wild-type *F. nucleatum* 12230 by oral gavage developed significantly more tumors in the colon than those inoculated with PBS, *E. coli*

DH5 α , or the *fadA*-deletion mutant US1 (Fig 7A), demonstrating a driver role of FadA in tumorigenesis. In all groups, significantly higher levels of *ANXA1* mRNA were detected in the tumors compared to the normal colonic tissues from the same mice, with the highest levels in the tumors induced by wild-type *F. nucleatum* (Fig 7B). These observations were consistent with our findings that *ANXA1* expression was increased in the proliferating cancerous cells (Fig 3A and B) and that FadA specifically induced *ANXA1* expression in those cells (Figs 4 and 6). A positive correlation between *fadA* and *ANXA1* was detected in *F. nucleatum*-induced tumors, with a correlation coefficient of 0.43 ($P = 0.01$; Fig 7C).

Among CRC patients, higher levels of *fadA* gene copy numbers and *ANXA1* mRNA were detected in the tumors than in the adjacent normal tissues by qPCR (Fig 7D and E), with a correlation coefficient of 0.62 ($P < 0.01$; Fig 7F). Immunofluorescent staining of paired tumor and normal tissues confirmed this finding, with significantly higher levels of FadA and Annexin A1 proteins detected in the tumors. Co-localization of FadA and Annexin A1 was observed in the tumors but not in the normal tissues (Fig 7G). Together, these results support the role of FadA and Annexin A1 in colorectal tumorigenesis.

FadA modulates β -catenin signaling in cancerous cells via Annexin A1

We have reported previously that binding of *F. nucleatum* to E-cadherin on CRC cells activates β -catenin signaling leading to over-expression of oncogenes such as Cyclin D1 (*CCND1*) [12]. When *ANXA1* was knocked down by siRNA, *F. nucleatum*-mediated activation of β -catenin expression was abolished in the cancerous 10C, HCT116, and DLD1 cells (Fig 8A). Nuclear translocation of β -catenin in 10C was also inhibited (Fig 8B). These data suggest Annexin A1 is required for activation of Wnt/ β -catenin signaling.

In 10C and HCT116 cells, Cyclin D1 gene expression also exhibited cell-density dependence, significantly higher in the non-confluent than confluent state, consistent with *ANXA1* expression (compare Figs 3A and 8C). In contrast, no expression difference was detected in the RKO cells where *ANXA1* was nearly undetectable (compare Figs 3A and 8C). However, when *ANXA1* was transfected into the RKO cells, Cyclin D1 expression was increased, indicating a driving role of Annexin A1 in oncogene expression (Fig 8D). These observations support the role of Annexin A1 in modulating β -catenin signaling.

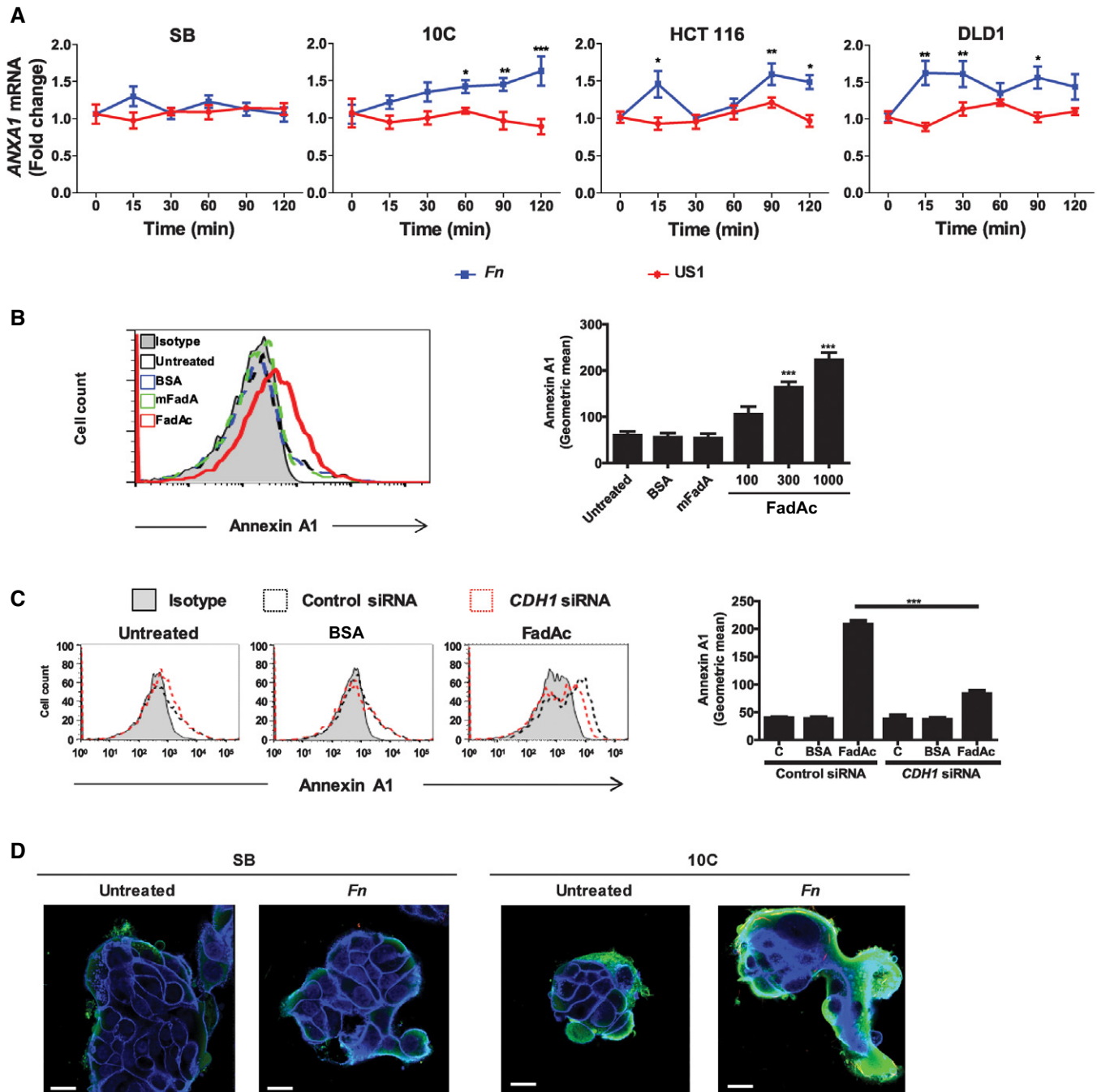


Figure 4. FadA induces Annexin A1 expression through E-cadherin.

- A** Real-time qPCR analysis of *ANXA1* mRNA levels in SB, 10C, HCT116, and DLD1 cells incubated with wild-type *F. nucleatum* 12230 (*Fn*) or *fadA*-deletion mutant US1 (US1) at MOI of 50:1 for the indicated time periods. The results were normalized to those obtained with untreated cells and were the mean of three independent experiments each performed in triplicates. Data are mean values \pm SEM. * $P < 0.05$, ** $P < 0.01$, and *** $P < 0.001$ (two-way ANOVA).
- B** Flow cytometry analysis of Annexin A1 expression in 10C cells either untreated, or incubated with BSA (1,000 $\mu\text{g/ml}$), or mFadA (1,000 $\mu\text{g/ml}$), or FadAc (100, 300, or 1,000 $\mu\text{g/ml}$) for 1 h. Data are mean values \pm SD. The experiment was performed in triplicates and repeated more than three times. *** $P < 0.001$ (one-way ANOVA).
- C** Flow cytometry analysis of Annexin A1 in 10C cells transfected with control siRNA (dotted black line) or *CDH1*-specific siRNA (dotted red line) followed by no treatment (untreated), or incubation with BSA (1,000 $\mu\text{g/ml}$) or FadAc (1,000 $\mu\text{g/ml}$) for 1 h. Data are mean values \pm SD. The experiment was performed in triplicates and repeated twice. *** $P < 0.001$ (two-way ANOVA).
- D** Confocal microscopy analysis of SB and 10C cells either untreated or following incubation with CFSE-labeled *F. nucleatum* 12230 (*Fn*) for 1 h at MOI of 5:1. Annexin A1 was stained green and E-cadherin blue. Images are 800 \times magnification. Note the enhanced expression of Annexin A1 in 10C compared to SB and its location on the outer layer of the cell mass. The experiment was repeated three times. Scale bar, 250 nm.

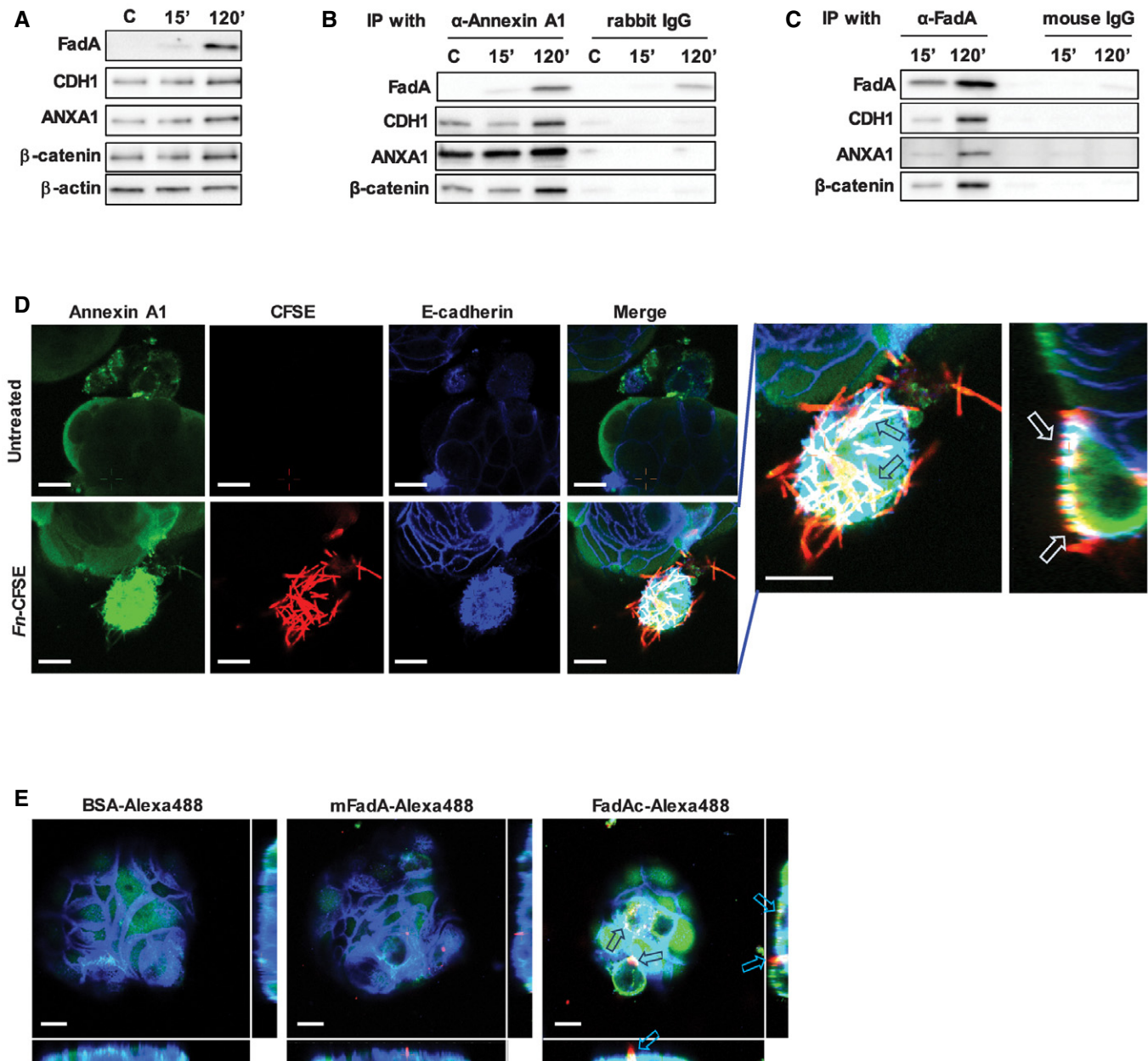


Figure 5. Fads, E-cadherin, Annexin A1, and β-catenin form a complex in cancerous cells.

- A Western blot analysis of Fads, E-cadherin (CDH1), Annexin A1 (ANXA1), and β-catenin in DLD1 cells following incubation with FadAc for 15 or 120 min. C, untreated cells. β-Actin was included as an internal control. The experiment was repeated three times.
- B Co-immunoprecipitation with Annexin A1. DLD1 cell lysates were incubated with FadAc for 15 or 120 min and then mixed with agarose beads conjugated with rabbit anti-Annexin A1 polyclonal antibody (α-Annexin A1) or control rabbit IgG. Fads, E-cadherin (CDH1), Annexin A1 (ANXA1), and β-catenin in the eluates were detected by Western blot. C, untreated control. The experiment was repeated three times.
- C Co-immunoprecipitation with Fads. DLD1 cell lysates were incubated with FadAc for 15 or 120 min and then mixed with agarose beads conjugated with mouse anti-Fads monoclonal antibody (α-Fads) or control mouse IgG. Fads, E-cadherin (CDH1), Annexin A1 (ANXA1), and β-catenin in the eluates were detected by Western blot. The experiment was repeated three times.
- D Confocal microscopy analysis of 10C cells either untreated (top panel) or following incubation with CFSE-labeled *F. nucleatum* 12230 (red, bottom panel) for 3 h and then immunofluorescent-stained for Annexin A1 (green) and E-cadherin (blue). Images are 1,200× magnification. A side view of the enlarged image is shown on the far right. Note the enhanced expression of Annexin A1 in the *F. nucleatum*-bound cells and the co-localization of Annexin A1, E-cadherin, and *F. nucleatum* on the cell membranes (arrows). The experiment was repeated more than three times. Scale bar, 500 nm.
- E Confocal microscopy analysis of 10C cells following incubation with Alexa Fluor™ 488-conjugated BSA, mFads, or FadAc (red) for 1 h followed by immunostaining of Annexin A1 (green) and E-cadherin (blue). Images are 1,200× magnification. Note the enhanced expression of Annexin A1 and its co-localization with E-cadherin in the presence of FadAc (arrows), but not with BSA or mFads. The experiment was repeated twice. The side views are shown to the right and bottom of each image. Scale bar, 500 nm.

Source data are available online for this figure.

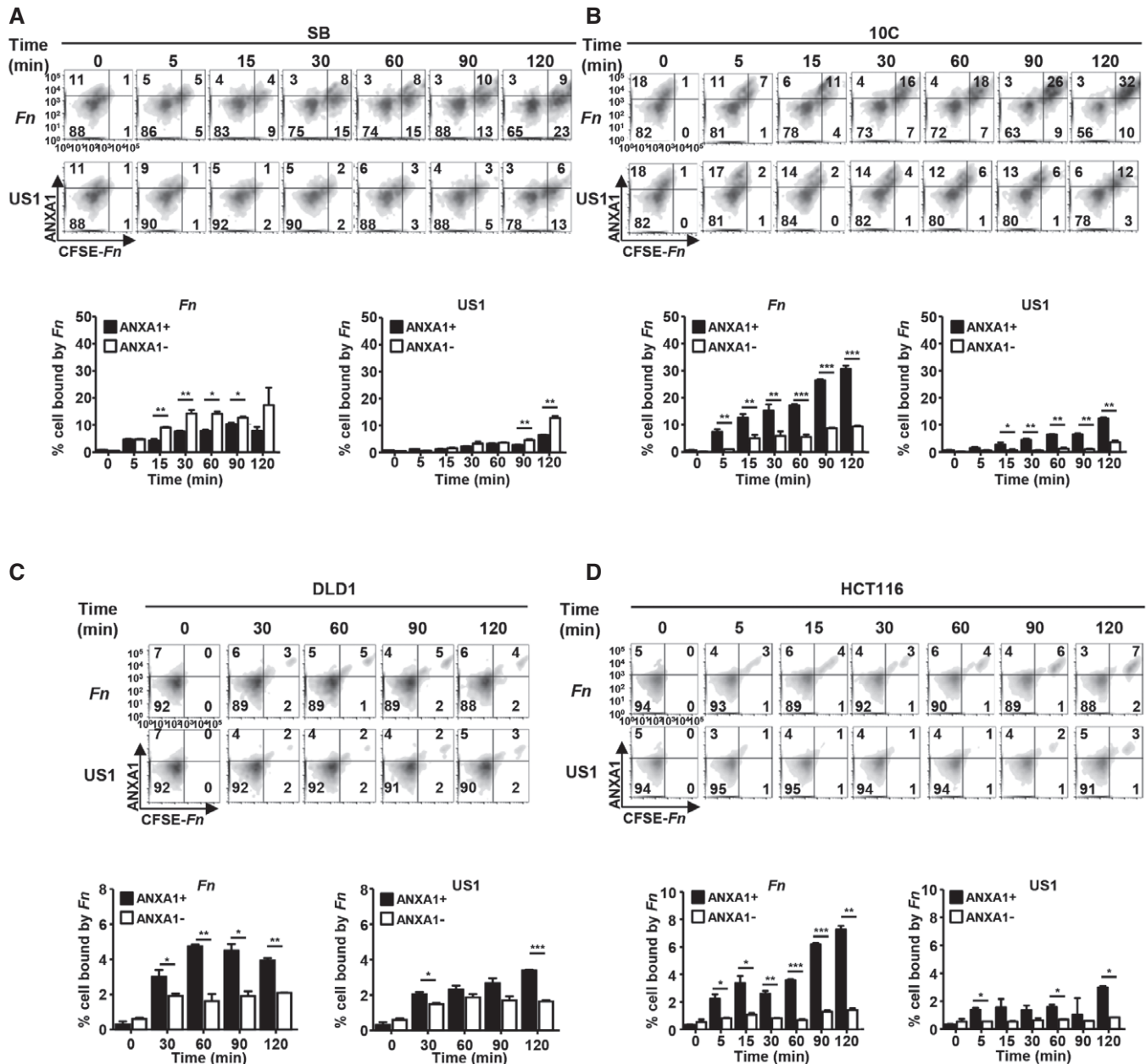


Figure 6. Positive feedback loop between FadA and Annexin A1.

A–D Flow cytometry analysis of SB (A), 10C (B), DLD1 (C), and HCT116 (D) cells incubated with CFSE-labeled *F. nucleatum* 12230 (Fn) or its *fadA*-deletion mutant US1 (US1) at MOI of 10–20:1 for the indicated time and immunostained with anti-Annexin A1 antibodies. Shown on the top panels are the density plots. x-axis, CFSE-labeled *F. nucleatum* or US1 (CFSE-Fn); y-axis, Annexin A1 (ANXA1). Shown on the bottom panels are the percentages of Annexin A1-positive (solid bars) or negative (clear bars) cells bound by *F. nucleatum* or US1 out of the total number of cells analyzed. Data are mean values \pm SD. The experiments were performed in triplicates and repeated 2–3 times. * $P < 0.05$, ** $P < 0.01$, *** $P < 0.001$ (two-way ANOVA).

Discussion

In this study, we elucidate the fundamental mechanistic difference between *F. nucleatum* interaction with the cancerous and non-cancerous cells. *F. nucleatum* preferentially binds to the cancerous cells, aided by Annexin A1, which is specifically expressed in proliferating CRC cells. This is consistent with our previous report that, although *F. nucleatum* is detected in both colorectal adenoma and

adenocarcinoma tissues, the *fadA* gene levels are significantly higher in the latter than the former [12]. Whereas *F. nucleatum* may not alter pre-cancerous cells to cancer, once the benign cells become cancerous, they express elevated levels of Annexin A1, through which *F. nucleatum* activates the Wnt/ β -catenin signaling and stimulates growth. Based on these results, we propose a “two-hit” model in colorectal carcinogenesis (Fig 9), with the accumulation of host driver mutation(s), e.g., increased expression of Annexin A1,

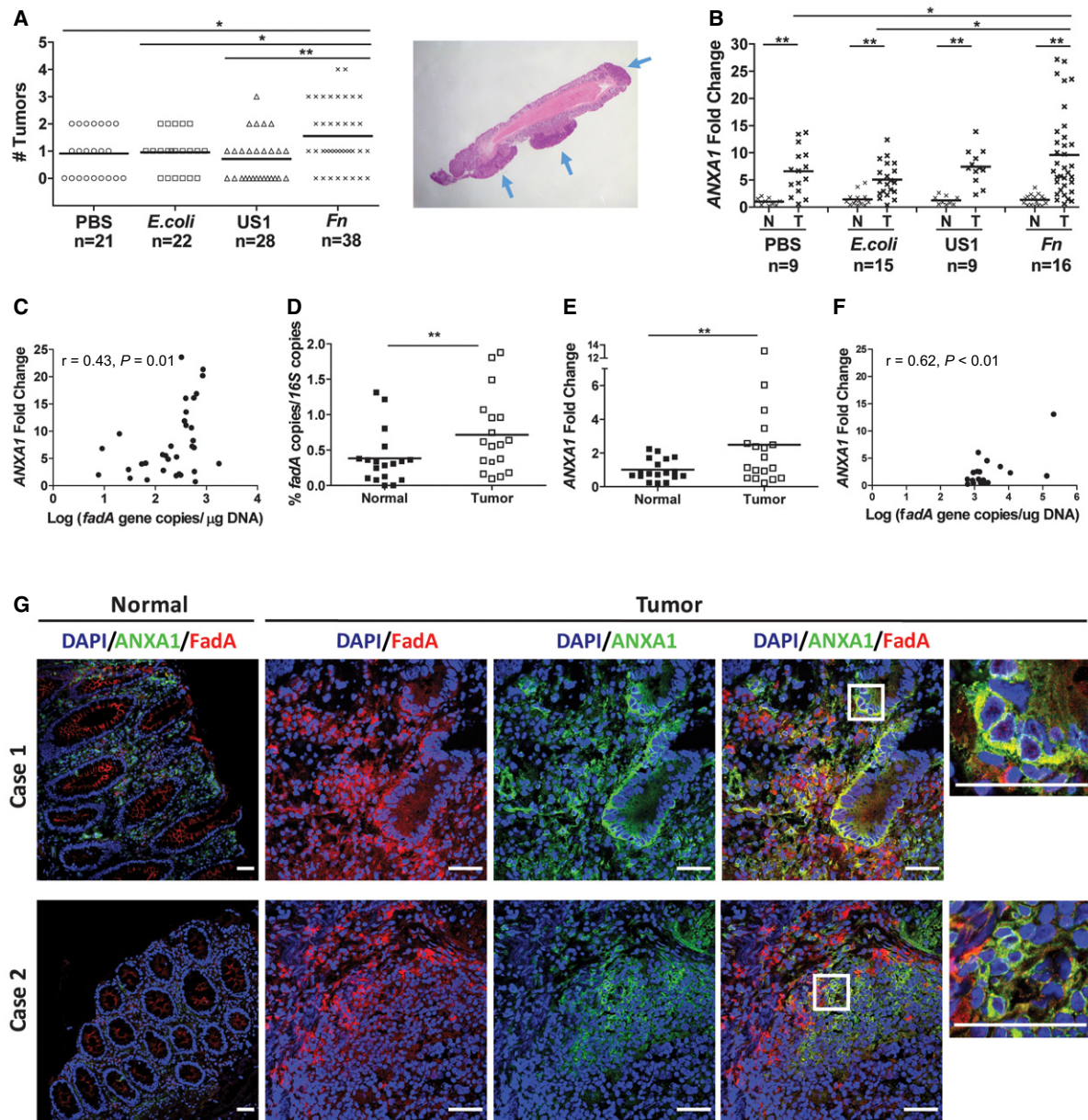


Figure 7. FadA and Annexin A1 co-express in colorectal tumors in mice and humans.

- A** Colorectal tumors generated in *Apc*^{min/+} mice following treatment with PBS, *E. coli* DH5α (*E. coli*), *fadA*-deletion mutant US1 (US1), or *F. nucleatum* 12230 (*Fn*). Each symbol represents one mouse. Horizontal lines represent mean values. Representative tumors formed in the mouse colon are shown on the right, pointed by blue arrows. * $P < 0.05$, ** $P < 0.01$ (one-way ANOVA).
- B** ANXA1 mRNA levels in *Apc*^{min/+} mouse paired normal colonic and tumor tissues as measured by real-time qPCR. Each symbol represents one mouse. Horizontal lines represent mean values. * $P < 0.05$, ** $P < 0.01$ (two-way ANOVA).
- C** Positive correlation between *fadA* gene copy numbers (x-axis) and ANXA1 mRNA levels (y-axis) in *F. nucleatum*-induced *Apc*^{min/+} mouse colonic tumors ($n = 34$; Pearson's correlation $r = 0.43, P = 0.01$). Each dot represents the average of qPCR results performed in duplicates.
- D** Abundance of *fadA* in the paired normal and adenocarcinoma tissues from human CRC patients ($n = 18$) expressed as ratio of *fadA* over total 16S rRNA genes determined by qPCR. Each symbol shows the average of duplicate qPCR results from one patient. Horizontal lines represent mean values. ** $P < 0.01$ (paired t-test).
- E** ANXA1 mRNA levels in paired normal and adenocarcinoma tissues from CRC patients ($n = 18$). Each symbol shows the average of duplicate qPCR results from one patient. Horizontal lines represent mean values. ** $P < 0.01$ (paired t-test).
- F** Positive correlation between *fadA* gene copy numbers (x-axis) and ANXA1 mRNA levels (y-axis) in human colorectal adenocarcinoma tissues ($n = 18$; Pearson's correlation $r = 0.62, P < 0.01$). Each dot represents the average of qPCR results performed in duplicates.
- G** Confocal microscopy analysis of paired normal and carcinoma tissues from two colon cancer patients. The frozen sections were incubated with rabbit anti-Annexin A1 polyclonal antibodies and 5G11 mouse anti-FadA monoclonal antibodies. The slides were then stained with Alexa Fluor[®] 680-conjugated donkey anti-rabbit and Alexa Fluor[®] 555-conjugated goat anti-mouse, washed, and covered in mounting medium containing DAPI. The scanning confocal microscopy images were taken with a Nikon Ti Eclipse inverted microscope at 200× magnification for the normal tissues and 400× for the carcinomas. Scale bar, 50 μm. Co-localization of FadA (red) and Annexin A1 (green) was observed in carcinomas but not in the paired normal tissues. See Fig EV5 for isotype (rabbit and mouse IgG) controls.

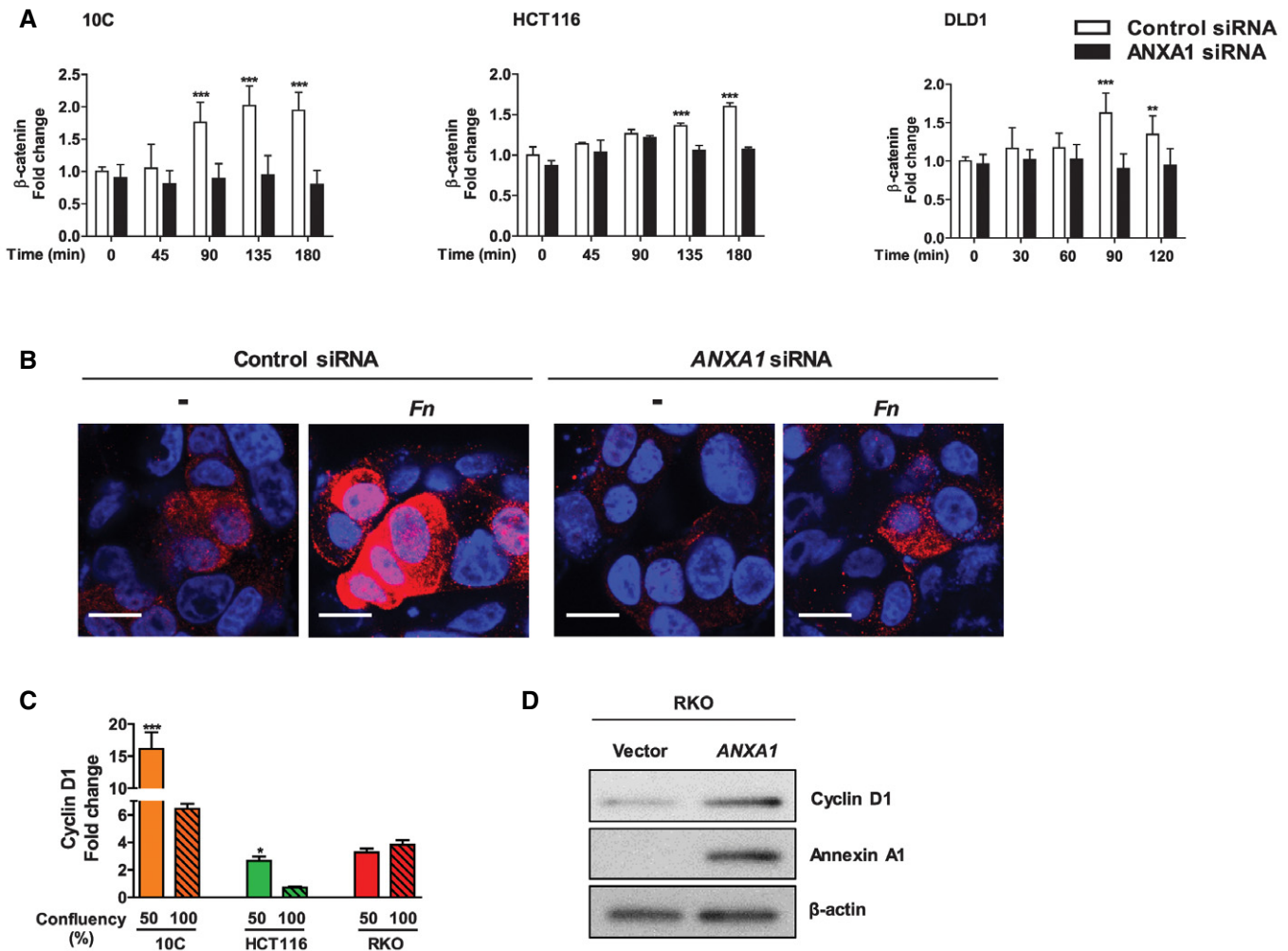


Figure 8. *Fusobacterium nucleatum* activates β -catenin signaling via Annexin A1.

- A** Flow cytometry analysis of β -catenin expression in 10C, HCT116, and DLD1 cells transfected with control siRNA (clear bars) or ANXA1-specific siRNA (solid bars) following incubation with *F. nucleatum* 12230 at MOI of ~20:1 for indicated time periods. The geometric means of cells treated with control siRNA at time 0 were designated as 1. Data are mean values \pm SD. The experiment was performed in duplicates or triplicates and repeated 1–3 times. $^{**}P < 0.01$, $^{***}P < 0.001$ (two-way ANOVA).
- B** Immunostaining of β -catenin in 10C cells transfected with control siRNA or ANXA1-specific siRNA following incubation with *F. nucleatum* 12230 (Fn) at MOI of ~100:1 for 2 h. β -Catenin was stained with Alexa Fluor[®] 680 (red) and the nuclei with DAPI (blue). The images were captured with confocal microscope at 800 \times magnification. -, no bacteria added. Note the increased expression of β -catenin and its nucleus translocation in response to *F. nucleatum* in control siRNA-treated cells, but not in ANXA1 siRNA-treated cells. The experiment was repeated twice. Scale bar, 200 nm.
- C** Real-time qPCR analysis of *CCND1* expression using mRNA extracted from the cancerous 10C, HCT116 and RKO, each grown to 50 or 100% confluency. Data are mean values \pm SEM. The experiment was performed in triplicates and repeated twice. $^{*}P < 0.05$, $^{***}P < 0.001$ (Student's *t*-test).
- D** Western blot analysis of Cyclin D1, Annexin A1, and β -actin in RKO cells transfected with control vector or ANXA1. Induction of Cyclin D1 was observed in response to transfection of Annexin A1. The experiment was repeated twice.

Source data are available online for this figure.

serving as the first “hit”, and microbes, e.g., *F. nucleatum*, as the second “hit” to exacerbate cancer progression. This model extends the well known “adenoma-carcinoma” model [38] identifying microbes as facilitators for CRC.

In support of the “two-hit” model, previous studies have reported microbes promoting cancer in predisposed hosts, i.e., after the “first hit” has occurred. For instance, enterotoxigenic *Bacteroides fragilis* and colibactin-producing *E. coli* are significantly enriched in the colonic mucus of individuals with familial adenomatous polyposis (FAP), who

are prone to developing CRC. These two microorganisms collaboratively enhance early tumorigenesis and mortality in the *Apc*^{min/+} mouse model [39]. *Salmonella enterica* serovar Typhi has been recognized as a significant risk factor for gallbladder cancer. It induces tumorigenesis in the *Apc*^{min/+} mouse model and malignant transformation in predisposed murine gallbladder organoids [40]. Although the virulence factors involved and the affected host signaling pathways may differ between the microbes and types of cancer, one commonality of the reported microbial-driven carcinogenesis is the predisposed host.

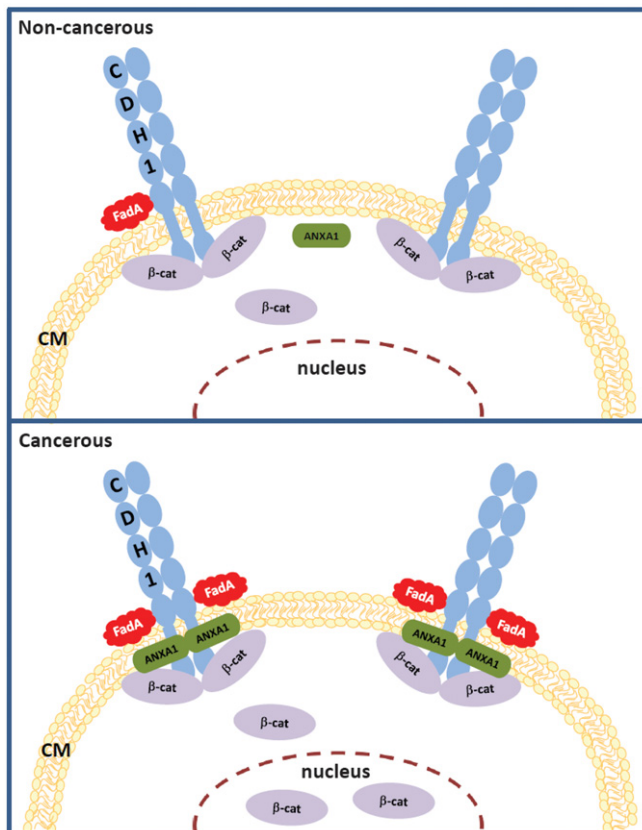


Figure 9. A “two-hit” model for CRC progression stimulated by *F. nucleatum*.

In non-cancerous cells (top panel), there is low level of Annexin A1 (ANXA1) and weak binding of FadA to E-cadherin (CDH1). In cancerous cells (bottom panel), Annexin A1 level increases, FadA binding enhances, FadA–E-cadherin–Annexin A1–β-catenin complex forms, β-catenin is activated, resulting in acceleration of cancer progression. CM, cell membrane.

In the case of *F. nucleatum*, stimulation of CRC is through an E-cadherin-mediated, positive feedback loop of FadA and Annexin A1, which is uniquely present in the cancerous cells, absent in the non-cancerous cells. Increased expression of Annexin A1 in the proliferating cancer cells enhances *F. nucleatum* binding, which in turn stimulates Annexin A1 expression and further enhances *F. nucleatum* binding and activates β-catenin signaling. We speculate that FadA binding to E-cadherin recruits Annexin A1 to the membrane to form a more stable complex, which may reduce cytoplasmic content of Annexin A1 thus stimulate compensatory overexpression of Annexin A1.

Our study elucidates Annexin A1 as a previously unrecognized modulator of Wnt/β-catenin signaling and a key growth factor of CRC. It is also a novel biomarker for colon cancer recurrence, independent of cancer stage, grade, age, and sex. Our study explains why CRC complicated with *F. nucleatum* has worse prognosis. Annexin A1 may be used in combination with cancer stage to improve the prognostic stratification of colon cancer patients. Approximately 75% of CRC are caused by mutations in the Wnt/β-catenin pathway [41]. However, Wnt/β-catenin signaling is involved in a broad spectrum of cellular functions. Due to such

complexity, so far no Wnt inhibitors have received FDA approval for cancer treatment [42]. Similarly, E-cadherin, through which *F. nucleatum* stimulates CRC [12], is also ubiquitous, rendering it an unsuitable therapeutic target, either. In contrast, Annexin A1, due to its selective expression in proliferating cancerous cells, is a promising therapeutic target. Inhibition of Annexin A1 suppresses β-catenin signaling in cancerous cells without affecting the non-cancerous cells, thus may have less adverse “off-target” effects.

F. nucleatum causes chemo-resistance in CRC and promotes metastasis [14,19], imposing a significant challenge to treatment. Antibiotic treatment is not desirable due to the risk of affecting the entire flora. A recent study indicates that Annexin A1 confers chemo-resistance in CRC [43]. It may be possible that *F. nucleatum* induces chemo-resistance through activating Annexin A1. Hence, Annexin A1 may be a target for overcoming chemo-resistance.

In short, to the best of our knowledge, this is the first study detailing the molecular mechanism of Annexin A1 in cancer and its interaction with cancer-stimulating microorganism. Given the broad implication of Wnt/β-catenin in cancer, and increasing numbers of reports of *F. nucleatum* in different types of cancer, Annexin A1 may be a novel therapeutic target for various cancers implicated with *F. nucleatum*. In addition, although Annexin A1 was identified through its interaction with *F. nucleatum*, we have demonstrated that it is a CRC growth factor independent of the microorganism. Its expression in other cancer types has been detected (Fig EV1A). Future studies will examine the role of Annexin A1 in different cancer types with or without *F. nucleatum*. Finally, our results of the cell-density-dependent expression of oncogenes suggest that subconfluent cells are useful for studying cancer gene regulations.

Materials and Methods

Bacterial strains and cell cultures

E. coli DH5α was grown at 37°C in LB broth in air. Wild-type *F. nucleatum* 12230 and its *fadA*-deletion mutant US1 were grown at 37°C in Columbia broth supplemented with 5 μg/ml hemin and 1 μg/ml menadione under anaerobic condition. To prepare CFSE-labeled *F. nucleatum*, the bacteria were incubated with 5-(and-6)-carboxy-fluorescein diacetate succinimidyl ester (CFSE; Invitrogen, Grand Island, NY), followed by enumeration on the blood agar plates. Cell cultures AA/C1 (aka C1), AA/C1/SB (aka SB), AA/C1/SB/10C (aka 10C), HCT116, DLD1, SW480, HT29, RKO, PC-9, 22RV1, UMUC3, and MCF-7 were maintained as previously described [12,32].

Plasmid construction and DNA/RNA transfections

Full-length *ANXA1* was amplified by PCR using primers listed in Table EV1 and cloned in to pcDNA™3.1 (+) Mammalian Expression Vector. Plasmid transfection was performed using Lipofectamine 2000 (Invitrogen, CA) following the manufacturer's instructions. Control siRNA, *ANXA1*-specific siRNA, and *CDH1*-specific siRNA were purchased from Invitrogen. Transfection of siRNA was performed using Lipofectamine RNAiMAX (Invitrogen) following the manufacturer's instructions.

Protein purification and conjugation

FadAc and mFadA were purified as previously described [22]. To conjugate, FadAc, mFadA, and BSA (MP Biomedicals, Santa Ana, CA) were mixed with Alexa Fluor™ 488 tetrafluorophenyl (TFP) ester (Invitrogen). Following reaction, unconjugated Alexa Fluor™ 488 TFP was removed using the PD-10 Desalting Column (GE Healthcare Life Sciences, Buckinghamshire, UK). The amount of labeled protein was quantified using a spectrophotometer (NanoDrop Technologies, Wilmington, DE).

Cell proliferation assay

Cells were seeded in 24-well plates and were untreated or incubated with bacteria at an MOI 1,000:1. The media were replaced, and fresh bacteria were added every 48 h. Cells were trypsinized, and cell numbers were counted using a hemocytometer as previously described [12]. Each experiment was performed in triplicate and repeated at least three times.

Cell culture attachment and invasion assay

The assay was performed as previously described [44]. Briefly, host cells were seeded in 24-well plates and allowed to grow till 80% confluent. The bacteria were then added at an MOI 50:1 followed by incubation for 1 h. Following washes with PBS and lysis with water, serial dilutions of the lysates were plated onto blood agar plates to enumerate the viable bacterial counts. For the invasion assay, bacteria were incubated with the host cells for 3 h followed by treatment with 300 µg/ml gentamicin and 200 µg/ml metronidazole for 1 h. After washes with PBS, the cells were lysed with water and intracellular bacterial counts were determined as described above. The levels of attachment and invasion were expressed as the percentage of bacteria recovered following cell lysis relative to the total number of bacteria initially added. Each experiment was performed in triplicate and repeated at least three times.

Flow cytometry

Cells were incubated with *F. nucleatum* or purified FadA for indicated time periods. After washing with PBS, the cells were collected and fixed with 75% cold ethanol. The cells were blocked with 2% skim milk followed by incubation with rabbit anti-Annexin A1 polyclonal IgG (Invitrogen), or rabbit anti-β-catenin polyclonal IgG (Invitrogen), or rabbit IgG isotype control (Invitrogen). The cells were then incubated with Alexa Fluor® 700-conjugated goat anti-rabbit IgG (Invitrogen), and the flow cytometric data were acquired by a BD LSR II flow cytometer and analyzed using FlowJo software (Tree Star, San Carlos, CA).

Clinical specimens

This study was approved by the Internal Review Board of Columbia University. A total of 18 CRC cases were retrieved from files at the Department of Pathology at Columbia University Medical Center. Hematoxylin and eosin (H&E) slides were reviewed to confirm the presence of colorectal adenocarcinoma. Frozen sections of the paired tumor and normal tissues were obtained for DNA/RNA extraction and immunofluorescent staining.

DNA and RNA extraction and real-time quantitative PCR (qPCR)

RNA was extracted from cultured cells using QIAGEN RNeasy Mini Kit. All Prep DNA/RNA Mini Kit was used to extract DNA and RNA from normal and tumor tissues from mice and clinical specimens. DNA and RNA concentrations were measured using NanoDrop ND 1000 spectrophotometer. Reverse transcription was performed using Superscript IV First-Strand Synthesis System (Invitrogen) following the manufacturer's instructions. Real-time qPCR was performed in StepOnePlus (Applied Biosystems, CA) in duplicates using primers listed in Table EV1. To quantify gene copies, standard curves using plasmids carrying 16S rRNA gene or *fadA* gene were generated. For RNA, data were analyzed using the $2(-\Delta\Delta Ct)$ method [45] and normalized to the β-actin control.

Immunofluorescent staining

Cells seeded into Nunc Lab-Tek II Chamber Slide System (Thermo Fisher Scientific, Waltham, MA) were incubated with CFSE-labeled *F. nucleatum* or Alexa Fluor™ 488-conjugated FadAc, mFadA, and BSA for indicated time periods. Following washes, the cells were fixed with 4% paraformaldehyde. After blocking with 2% skim milk and 0.3% Triton X-100, the cells were incubated with goat anti-human E-cadherin polyclonal antibodies (R&D Systems, MN) and rabbit anti-Annexin A1 polyclonal antibodies (Invitrogen) or rabbit anti-β-catenin polyclonal IgG (Invitrogen). After washing, the cells were incubated with Cy3-conjugated donkey anti-goat IgG (Jackson ImmunoResearch, West Grove, PA) and Alexa Fluor® 680-conjugated donkey anti-rabbit IgG (Invitrogen), washed, and covered in mounting medium containing DAPI (Vector Laboratories, Burlingame, CA). The samples were visualized with a Nikon Ti Eclipse inverted microscope for scanning confocal microscopy.

For immunofluorescent staining of human colonic specimens, frozen sections of the paired tumor and normal tissues were fixed in 4% paraformaldehyde for 15 min, and permeabilized using 0.1% Triton X-100 in PBS followed by blocking of non-specific binding. The slides were then incubated with rabbit anti-Annexin A1 polyclonal antibodies (Thermo Fisher Scientific) and mouse anti-FadA monoclonal antibody 5G11 [22], or with isotype controls of rabbit IgG (Invitrogen) and mouse IgG (R&D Systems, Minneapolis, MN). After washes, the slides were incubated with Alexa Fluor® 680-conjugated donkey anti-rabbit (Invitrogen) and Alexa Fluor® 555-conjugated goat anti-mouse (Invitrogen), washed, and covered in mounting medium containing DAPI. The slides were visualized as above.

Western-blot analysis

RKO cells transfected with *ANXA1* expression vector or expression vector alone were seeded in 6-well plates and grown for 2 days. The cells were washed with ice-cold PBS and lysed with RIPA lysis buffer (EMD Millipore, Burlington, MA) containing Halt™ Protease and Phosphatase Inhibitor Single-Use Cocktail (Thermo Fisher Scientific). The cell lysates were centrifuged at $13,000 \times g$ for 10 min at 4°C, and the protein concentration was measured using the BCA Protein Assay Kit (Thermo Fisher Scientific) according to the manufacturer's instructions. One microgram of total proteins was separated by NuPAGE™ 4-12% Bis-Tris Gel (Thermo Fisher

Scientific) and transferred onto PVDF membranes (Bio-Rad, Hercules, CA). The membrane was blocked with 5% skim milk in TBS containing 0.1% Tween-20 (TBST) at room temperature for 1 h followed by incubation with antibodies against Annexin A1 (Thermo Fisher Scientific, 71-3400, 1:4,000 dilution), Cyclin D1 (Thermo Fisher, Cat No 701421, 1:250 dilution), β -catenin (Thermo Fisher Scientific, 71-2700, 1:2,000 dilution), or β -actin (Abcam, ab6276, 1:4,000 dilution) in 0.5% skim milk in TBST at 4°C overnight. After washing three times with TBST, the membrane was incubated with HRP-conjugated secondary antibody in TBST at room temperature for 1 h. The immune reactive bands were detected with ECL Western Blotting Substrate (Thermo Fisher Scientific).

Co-immunoprecipitation

DLD1 cells were incubated with 1 mg/ml of FadAc for 0, 15, and 120 min, respectively. Rabbit anti-Annexin A1 antibody (Thermo Fisher Scientific), mouse anti-FadA antibody 5G11 [22], rabbit IgG, or mouse IgG were bound covalently to the agarose resins using the Pierce Co-Immunoprecipitation Kit (Thermo Fisher Scientific) following the manufacturer's instructions. The cells were lysed and mixed with the antibody-coupled resins and incubated for 2 h at room temperature. Following washes, the complex bound to the antibodies was eluted and examined by Western blot analysis as described above. Following electrophoresis and transfer, the PVDF membranes were incubated with rabbit anti-Annexin A1 polyclonal antibodies (Thermo Fisher Scientific), mouse anti-FadA monoclonal antibodies 7H7, rabbit anti-E-cadherin monoclonal antibodies (Cell Signaling Technology), mouse anti- β -actin monoclonal antibodies (Cell Signaling Technology), or rabbit anti- β -catenin polyclonal antibodies (Thermo Fisher Scientific). After washes, the membranes were incubated with HRP-conjugated goat anti-rabbit IgG antibodies (Bio-Rad) or Poly-HRP-conjugated goat anti-mouse IgG antibodies (Thermo Fisher Scientific). The membranes were washed and incubated with SuperSignal West Pico Chemiluminescent Substrate (Thermo Fisher Scientific) and the bands were detected using ChemiDoc MP Imaging System (Bio-Rad).

Apc^{min/+} mouse model

The animal protocol was approved by the Columbia University Institutional Animal Care and Use Committee (New York, NY). All mice were kept in sterilized filtered-topped cages in a room with 12-h light cycle, fed autoclaved food and water *ad libitum*, and handled in a laminar flow hood. Prior to bacterial inoculation, the mice (both male and female) were provided with antibiotic-supplemented drinking water for 2 weeks. Bacteria cultures were re-suspended in PBS to an estimated density of 2×10^{10} CFU/ml. An aliquot of 50 μ l of the bacterial suspension was gavaged three times a week for 8 weeks. At the end of the treatment, animals were sacrificed and the tumors in the colon were counted. Tumors and normal intestinal tissues were collected for histological analysis and extraction of DNA and RNA.

Tumor xenografts

Four-week-old female nude mice were purchased from Taconic Biosciences (NY, USA). An inoculum of 1×10^7 HCT116 or DLD1 cells

treated with either control or *ANXA1*-specific siRNA was injected subcutaneously and bilaterally into the nude mice, with control cells injected on the left side and *ANXA1*-knockdown cells on the right side. After 7–9 days, the tumor length and width were measured using calipers and tumor volumes were calculated using the following formula: Volume = (width)² \times length/2. The results are expressed as percentage of the size of the control siRNA-transfected tumor.

Statistical analysis

The differences between groups were examined by two-tailed *t*-test, and one-way or two-way ANOVA followed by the Student–Newman–Keuls (SNK) tests. *P* < 0.05 was considered statistically significant.

Statistical analysis of associations between exposure to *F. nucleatum* and up-regulation of *ANXA1* mRNA expression levels in colon cancer cell HT29

The relationship between exposure of colon cancer cells to *F. nucleatum* and up-regulation of *ANXA1* mRNA expression levels was investigated in an RNA-sequencing (RNA-seq) dataset publicly available from the NCBI-GEO online repository (GSE090944) and containing global gene-expression measurements from HT29 cells, both at baseline and following infection with *F. nucleatum*, in triplicates [14]. The distribution of *ANXA1* mRNA expression levels in the two sample groups (baseline versus infected) was visualized using boxplots, using the log₂ of their TPM (*transcripts per million*) expression values as a metric. Differences in mean log₂ TPM values between HT29 cells at baseline (*n* = 3) and following incubation with *F. nucleatum* (*n* = 3) were tested for statistical significance using a two-tailed *t*-test for continuous variables.

Statistical analysis of associations between *ANXA1* expression levels and survival outcomes in colon cancer patients

The relationship between *ANXA1* mRNA expression levels and *disease-free survival* (DFS) was investigated in a database of 466 primary colon carcinomas, assembled by pooling four independent gene-expression microarray datasets downloaded from the NCBI-GEO online repository (GSE14333, GSE17538, GSE31595, GSE37892), as previously described [34]. To evaluate whether differences in *ANXA1* mRNA expression levels between different tumor samples might have been grossly distorted by differences in each sample's relative content of epithelial cells (i.e., tumor cell density), *ANXA1* mRNA expression levels (Affymetrix probe: 201012_at) were plotted against those of an epithelial-specific reference marker, such as *DSP* (Desmoplakin; Affymetrix probe: 200606_at), and visually inspected to exclude meaningful correlations. The association between *ANXA1* mRNA expression levels and DFS was visualized using Kaplan–Meier survival curves, after patient stratification in groups with high, medium and low *ANXA1* expression levels, using three different methods: (i) based on the median of *ANXA1* expression levels (bottom 50% versus top 50%); (ii) based on the quartile distribution of *ANXA1* expression levels (bottom 25% versus middle 50% versus top 25%); and (iii) based on *ANXA1* expression thresholds calculated using the StepMiner algorithm (low versus high), and adopting as definition of the

boundary between low and high levels, the \log_2 value of *ANXA1* normalized expression levels corresponding to StepMiner + 0.5, as previously described [35,36]. Differences in survival rates between patient subgroups were tested for statistical significance using the log-rank test. The association between high levels of *ANXA1* mRNA expression and increased risk of recurrence was also tested using univariate and multivariate analyses based on the Cox proportional hazards method, in which *ANXA1* mRNA expression levels were modeled as a continuous variable. The analyses were first conducted across the whole database ($n = 466$) and subsequently in the subset of patients that were also annotated with the pathological grading of the respective tumors ($n = 216$), as previously described [34]. The multivariate analysis was aimed at excluding possible confounding effects from clinical stage, pathological grade, age, or sex. Hazard ratios (HRs) were tested for statistical significance (null hypothesis: HR = 1) using the Wald test.

Expanded View for this article is available online.

Acknowledgements

We thank Dr. Ann C. Williams for generously providing the AA/C1, AA/C1/SB, and AA/C1/SB/10C cell lines, Dr. Swarnali Acharyya for the PC-9 cell line, and Dr. Cory T. Abate-Shen for the 22RV1 and UMUC3 cell lines. This work was supported in part by NIH grants R01CA192111 to Y.W.H. and T.C.W., and R01DE014924 and R01DE023332 to Y.W.H., as well as Damon Runyon-Rachleff Innovation Award DRR-44-16 from the Damon Runyon Cancer Research Foundation to P.D. Images were collected, and image processing and analysis for this work were performed in the Confocal and Specialized Microscopy Shared Resource of the Herbert Irving Comprehensive Cancer Center at Columbia University, supported by NIH grant # P30 CA013696.

Author contributions

YWH conceived, designed, and supervised the study. MRR, JEB, RPH, WJR, DS, and PD performed the study. SML provided clinical specimens. YWH, MRR, JEB, SML, PD, and TCW interpreted the results. YWH, MRR, JEB, and PD wrote the manuscript.

Conflict of interest

P.D. receives royalties and/or stocks from OncoMed Pharmaceuticals, Inc., Quantical Pharmaceuticals, Inc. (now a fully owned subsidiary of Celgene), and Forty Seven, Inc. as a co-inventor of several patents and patent applications.

References

1. ACS (2012) Cancer Facts & Figures 2012. In pp 1–66. American Cancer Society (ACS)
2. Vogelstein B, Kinzler KW (1993) The multistep nature of cancer. *Trends Genet* 9: 138–141
3. Abreu MT, Peek Jr RM (2014) Gastrointestinal malignancy and the microbiome. *Gastroenterology* 146: 1534–1546.e3
4. Akkari L, Gocheva V, Kester JC, Hunter KE, Quick ML, Sevenich L, Wang HW, Peters C, Tang LH, Klimstra DS et al (2014) Distinct functions of macrophage-derived and cancer cell-derived cathepsin Z combine to promote tumor malignancy via interactions with the extracellular matrix. *Genes Dev* 28: 2134–2150
5. Schwabe RF, Jobin C (2013) The microbiome and cancer. *Nat Rev Cancer* 13: 800–812
6. Dulal S, Keku TO (2014) Gut microbiome and colorectal adenomas. *Cancer J* 20: 225–231
7. Keku TO, Dulal S, Deveaux A, Jovov B, Han X (2015) The gastrointestinal microbiota and colorectal cancer. *Am J Physiol Gastrointest Liver Physiol* 308: G351–G363
8. Keku TO, McCoy AN, Azcarate-Peril AM (2013) *Fusobacterium* spp. and colorectal cancer: cause or consequence? *Trends Microbiol* 21: 506–508
9. McCoy AN, Araujo-Perez F, Azcarate-Peril A, Yeh JJ, Sandler RS, Keku TO (2013) *Fusobacterium* is associated with colorectal adenomas. *PLoS ONE* 8: e53653
10. Kostic AD, Chun E, Robertson L, Glickman JN, Gallini CA, Michaud M, Clancy TE, Chung DC, Lochhead P, Hold GL et al (2013) *Fusobacterium nucleatum* potentiates intestinal tumorigenesis and modulates the tumor-immune microenvironment. *Cell Host Microbe* 14: 207–215
11. Kostic AD, Gevers D, Pedamallu CS, Michaud M, Duke F, Earl AM, Ojesina AI, Jung J, Bass AJ, Taberero J et al (2012) Genomic analysis identifies association of *Fusobacterium* with colorectal carcinoma. *Genome Res* 22: 292–298
12. Rubinstein MR, Wang X, Liu W, Hao Y, Cai G, Han YW (2013) *Fusobacterium nucleatum* promotes colorectal carcinogenesis by modulating E-cadherin/ β -catenin signaling via its FadA adhesin. *Cell Host Microbe* 14: 195–206
13. Gur C, Ibrahim Y, Isaacson B, Yamin R, Abed J, Gamliel M, Enk J, Bar-On Y, Stanitsky-Kaynan N, Copenhagen-Glazer S et al (2015) Binding of the Fap2 protein of *Fusobacterium nucleatum* to human inhibitory receptor TIGIT protects tumors from immune cell attack. *Immunity* 42: 344–355
14. Yu T, Guo F, Yu Y, Sun T, Ma D, Han J, Qian Y, Kryczek I, Sun D, Nagarsheth N et al (2017) *Fusobacterium nucleatum* promotes chemoresistance to colorectal cancer by modulating autophagy. *Cell* 170: 548–563.e16
15. Tahara T, Yamamoto E, Suzuki H, Maruyama R, Chung W, Garriga J, Jelinek J, Yamano HO, Sugai T, An B et al (2014) *Fusobacterium* in colonic flora and molecular features of colorectal carcinoma. *Can Res* 74: 1311–1318
16. Mima K, Cao Y, Chan AT, Qian ZR, Nowak JA, Masugi Y, Shi Y, Song M, da Silva A, Gu M et al (2016) *Fusobacterium nucleatum* in colorectal carcinoma tissue according to tumor location. *Clin Transl Gastroenterol* 7: e200
17. Yu J, Chen Y, Fu X, Zhou X, Peng Y, Shi L, Chen T, Wu Y (2016) Invasive *Fusobacterium nucleatum* may play a role in the carcinogenesis of proximal colon cancer through the serrated neoplasia pathway. *Int J Cancer* 139: 1318–1326
18. Mima K, Nishihara R, Qian ZR, Cao Y, Sukawa Y, Nowak JA, Yang J, Dou R, Masugi Y, Song M et al (2016) *Fusobacterium nucleatum* in colorectal carcinoma tissue and patient prognosis. *Gut* 65: 1973–1980
19. Bullman S, Pedamallu CS, Sicinska E, Clancy TE, Zhang X, Cai D, Neuberg D, Huang K, Guevara F, Nelson T et al (2017) Analysis of *Fusobacterium* persistence and antibiotic response in colorectal cancer. *Science* 358: 1443–1448
20. Flanagan L, Schmid J, Ebert M, Soucek P, Kunicka T, Liska V, Bruha J, Neary P, Dezeuw N, Tommasino M et al (2014) *Fusobacterium nucleatum* associates with stages of colorectal neoplasia development, colorectal cancer and disease outcome. *Eur J Clin Microbiol Infect Dis* 33: 1381–1390
21. Abed J, Emgard JE, Zamir G, Faroja M, Almogly G, Grenov A, Sol A, Naor R, Pikarsky E, Atlan KA et al (2016) Fap2 mediates *Fusobacterium*

- nucleatum* colorectal adenocarcinoma enrichment by binding to tumor-expressed Gal-GalNAc. *Cell Host Microbe* 20: 215–225
22. Xu M, Yamada M, Li M, Liu H, Chen SG, Han YW (2007) FadA from *Fusobacterium nucleatum* utilizes both secreted and nonsecreted forms for functional oligomerization for attachment and invasion of host cells. *J Biol Chem* 282: 25000–25009
23. Gerke V, Moss SE (2002) Annexins: from structure to function. *Physiol Rev* 82: 331–371
24. Guo C, Liu S, Sun MZ (2013) Potential role of Anxa1 in cancer. *Fut Oncol* 9: 1773–1793
25. Boudhraa Z, Bouchon B, Viallard C, D'Incan M, Degoul F (2016) Annexin A1 localization and its relevance to cancer. *Clin Sci* 130: 205–220
26. Su N, Xu XY, Chen H, Gao WC, Ruan CP, Wang Q, Sun YP (2010) Increased expression of annexin A1 is correlated with K-ras mutation in colorectal cancer. *Tohoku J Exp Med* 222: 243–250
27. Duncan R, Carpenter B, Main LC, Telfer C, Murray GI (2008) Characterisation and protein expression profiling of annexins in colorectal cancer. *Br J Cancer* 98: 426–433
28. Shimoyama Y, Nagafuchi A, Fujita S, Gotoh M, Takeichi M, Tsukita S, Hirohashi S (1992) Cadherin dysfunction in a human cancer cell line: possible involvement of loss of alpha-catenin expression in reduced cell-cell adhesiveness. *Can Res* 52: 5770–5774
29. Tiang JM, Butcher NJ, Cullinane C, Humbert PO, Minchin RF (2011) RNAi-mediated knock-down of arylamine N-acetyltransferase-1 expression induces E-cadherin up-regulation and cell-cell contact growth inhibition. *PLoS ONE* 6: e17031
30. Luo Y, Zhu YT, Ma LL, Pang SY, Wei LJ, Lei CY, He CW, Tan WL (2016) Characteristics of bladder transitional cell carcinoma with E-cadherin and N-cadherin double-negative expression. *Oncol Lett* 12: 530–536
31. Chao YL, Shepard CR, Wells A (2010) Breast carcinoma cells re-express E-cadherin during mesenchymal to epithelial reverting transition. *Mol Cancer* 9: 179
32. Williams AC, Harper SJ, Paraskeva C (1990) Neoplastic transformation of a human colonic epithelial cell line: *in vitro* evidence for the adenoma to carcinoma sequence. *Can Res* 50: 4724–4730
33. Roth U, Razawi H, Hommer J, Engelmann K, Schwientek T, Muller S, Baldus SE, Patsos G, Corfield AP, Paraskeva C et al (2010) Differential expression proteomics of human colorectal cancer based on a syngeneic cellular model for the progression of adenoma to carcinoma. *Proteomics* 10: 194–202
34. Dalerba P, Sahoo D, Paik S, Guo X, Yothers G, Song N, Wilcox-Fogel N, Forgo E, Rajendran PS, Miranda SP et al (2016) CDX2 as a prognostic biomarker in stage II and stage III colon cancer. *N Engl J Med* 374: 211–222
35. Dalerba P, Kalisky T, Sahoo D, Rajendran PS, Rothenberg ME, Leyrat AA, Sim S, Okamoto J, Johnston DM, Qian D et al (2011) Single-cell dissection of transcriptional heterogeneity in human colon tumors. *Nat Biotechnol* 29: 1120–1127
36. Sahoo D, Dill DL, Tibshirani R, Plevritis SK (2007) Extracting binary signals from microarray time-course data. *Nucleic Acids Res* 35: 3705–3712
37. Fardini Y, Wang X, Temoin S, Nithianantham S, Lee D, Shoham M, Han YW (2011) *Fusobacterium nucleatum* adhesin FadA binds vascular endothelial cadherin and alters endothelial integrity. *Mol Microbiol* 82: 1468–1480
38. Fearon ER, Vogelstein B (1990) A genetic model for colorectal tumorigenesis. *Cell* 61: 759–767
39. Dejea CM, Fathi P, Craig JM, Boleij A, Taddese R, Geis AL, Wu X, DeStefano Shields CE, Hechenbleikner EM, Huso DL et al (2018) Patients with familial adenomatous polyposis harbor colonic biofilms containing tumorigenic bacteria. *Science* 359: 592–597
40. Scanu T, Spaapen RM, Bakker JM, Pratap CB, Wu LE, Hofland I, Broeks A, Shukla VK, Kumar M, Janssen H et al (2015) Salmonella manipulation of host signaling pathways provokes cellular transformation associated with gallbladder carcinoma. *Cell Host Microbe* 17: 763–774
41. Novellasedumunt L, Antas P, Li VS (2015) Targeting Wnt signaling in colorectal cancer. A review in the theme: cell signaling: proteins, pathways and mechanisms. *Am J Physiol Cell Physiol* 309: C511–C521
42. Krishnamurthy N, Kurzrock R (2018) Targeting the Wnt/beta-catenin pathway in cancer: update on effectors and inhibitors. *Cancer Treat Rev* 62: 50–60
43. Onozawa H, Saito M, Saito K, Kanke Y, Watanabe Y, Hayase S, Sakamoto W, Ishigame T, Momma T, Ohki S et al (2017) Annexin A1 is involved in resistance to 5-FU in colon cancer cells. *Oncol Rep* 37: 235–240
44. Han YW, Shi W, Huang GT, Kinder Haake S, Park NH, Kuramitsu H, Genco RJ (2000) Interactions between periodontal bacteria and human oral epithelial cells: *Fusobacterium nucleatum* adheres to and invades epithelial cells. *Infect Immun* 68: 3140–3146
45. Livak KJ, Schmittgen TD (2001) Analysis of relative gene expression data using real-time quantitative PCR and the 2(-Delta Delta C(T)) Method. *Methods* 25: 402–408